Spring Test for Automatic Measuring of Signal Complexity

Jie Cheng (20204228009@stu.suda.edu.cn)
Soochow University https://orcid.org/0000-0002-6103-1893
Haiyong Huang
Soochow University
Wenshi Li
Soochow University https://orcid.org/0000-0002-6467-8449

Research Article

Keywords: Signal complexity measure automation, Spring test, Manifold metrics, Extreme value method, Phase detection

Posted Date: April 19th, 2022

DOI: https://doi.org/10.21203/rs.3.rs-1552057/v1

Spring Test for Automatic Measuring of Signal Complexity

Abstract --- In order to automatically measure the complexity of time series, we invented 3*S* plot, and the embedded spring is a one-dimensional manifold. Three automatic statistical indexes are defined by self-similarity measure, extreme value search acceleration and neighborhood rotation phase, respectively. The above three new metrics and another two comparison standards, Lyapunov exponent and spectral entropy complexity, can pass the benchmark system test of unified equation. Under the guidance of visualization of bifurcation diagram, three probability measuring methods with relatively weak independent recognition abilities and one phase measuring method with relatively sensitive detection ability can easily identify the order and chaos states following Chua's equation. Finally, five main measuring tools are used to successfully characterize the new 555 timer-based chaotic signals.

Key words --- Signal complexity measure automation; Spring test; Manifold metrics; Extreme value method; Phase detection.

I. Introduction

The complexity of system can generally be mined from the characteristics of its output data [1]. The premise is that measurable data is embedded with information, which is easy to be characterized by complexity metrics.

As an object to be identified, chaotic data flow widely born in meteorology, finance, brain science and circuitry often needs to measure there complexities, which can be regarded as complex information between order and random[2]. However, the automatic measure of complexity for embedding quasi random chaotic information has always been an open problem, and its new trend of the solution is data driven[3].

To summarize and understand the complexity theory of chaotic flow, which includes: (1) The view of symmetry breaking, which holds that the system complexity originates from symmetry breaking mechanism (A. M. Turing, 1952)[4]; (2) KAM theorem (1954-1963) suggests that orbital instability is the basic cause of chaos in the system[5]; (3) The maximum entropy principle (E. T. Jaynes, 1957)[6] suggests that while estimating information entropy, we concern both orbit ergodicity and metric transitivity; (4) The re-injection principle (O. E. Rössler, 1976)[7] outlines that chaotic mechanism is of Birkhoff's recurrent motions between Poincaré's cross-sections; (5) Takens embedding theorem (1981)[8] points out that the nonlinear characteristics of time series can be expressed as singular attractors in reconstructed phase space through the time delay and dimension raising (by derivatives and coordinates)(N. H. Packard, 1980); And (6) local activity theory (L. O. Chua, 2005)[9], the source of complexity is rooted in local activities. Focusing the equilibrium points of differential equation, the scalar product of the perturbation components of the nonlinear term and its related variables is calculated, and the integral is less than zero.

To digest key literatures[10,11] further, we note that: Strictly starting from probability, we need to obtain the probability density distribution in advance; Geometry is hard while manifolds are soft. Therefore, the research feeling (hypothesis) is that along the data track (based on track tracing), principle driven and computing driven need to be combined with data driven, so as to form the general strategy of automatic measuring for the complexity of time series.

In next part of key measuring review, the calculation methods outline five research perspectives (geometry, track entropy, Euclidean distance, total variation of track and total variation of track phase). Chua's equation is test example with its bifurcation diagram as the visual analysis background of chaotic evolution.

Into part of data-driven modeling techniques, five research tools are illustrated in detail, in which *LE* (Lyapunov exponent)[12,13] is the traditional detection index for chaos, *SEC* (spectral entropy complexity)[14,15] is coined as the gold standard for complexity measuring, our spring test metrics depict spring manifold, and the strict test case uses the unified equation.

Different from the above description in verification of nonlinear complex data from chaotic equations, in new case study, the 555 time-based chaotic identification pays attention to the application of three new criteria of spring test.

II. Methodology

Basic measuring methods review covers five features from track probability to track phase. In part of spring test metrics we present eight formulas from three characteristic perspectives of track family, FFT and our one dimensional manifold. Three test cases use two known chaos equations and one new chaos circuit based on 555-timer.

1. Basic measuring methods review

Six feature formulas introduce bifurcation diagram, track entropy, Euclidean distance, total variation of track and total variation of track phase, respectively.

1) Bifurcation diagram

The concept of bifurcation came from Poincaré in 1885. Drawing pseudo code flow chart of bifurcation diagram[16] by extreme value method is written in Formula 1:

$$\{y\} = \text{stacking}(findpeaks(x_{i,\ parameter})),\ parameter = [para_1, para_2] \tag{1}$$

Wherein the parameter scanning rang is from $para_1$ to $para_2$. The bifurcation diagram contributes magic film, in which the respiratory dynamics between order and chaos is uncovered by a gradual change of key parameter.

2) Track entropy

Formula 2 is mainly in form of Shannon entropy[17-19], which is applied here as track entropy.

$$E = \frac{-\sum_{i=1}^{N} p_i \ln p_i}{\ln N} \tag{2}$$

Wherein x_i is the i th value of normalized time series under test, track probability is written as $p_i=x_i/x_{max}$ and N is the data length.

3) Euclidean distance

The Euclidean distance D[20,21] is actually the sum of the difference squares measuring micro distances between the track probabilities and its average probability, be written in Formula 3.

$$D = \frac{\sum_{i=1}^{N} (p_i - \frac{1}{N})^2}{\ln N} \tag{3}$$

4) Total variation of track

The total variation of the track probability is coined as M in Formula 4, as the essence of probability measure[22], which is the sum of x_i differences.

$$M = \sum_{i=1}^{N\text{-}1} (x_{i+1} - x_i) \tag{4}$$

5) Total variation of track phase

The total variation of the track phase is recorded as P (meaning phase), as the basic characterization of phase dynamics[23,24], which is the sum of phase differences at adjacent points of the track (see Formula 5 and Formula 6).

$$v_i = \frac{\sum_{j=1}^{m} X_{i,j} X_{i+1,j}}{\sqrt{\sum_{j=1}^{m} (X_{i,j})^2} \sqrt{\sum_{j=1}^{m} (X_{i+1,j})^2}} \tag{5}$$

$$P = \sum_{i=1}^{N\text{-}1} (v_{i+1} - v_i) \tag{6}$$

2. Main measuring methods and the spring test

There exist two comparison standards, in which Lyapunov exponent (*LE*) is the golden criterion of chaos while spectral entropy complexity (*SEC*) can be considered as the golden criterion for complexity measure. Along the technical route of *SEC* without manual selection, three metrics of our invention noted spring test are proposed in detail.

1) Lyapunov exponent

As a positive maximum, *LE* is an important strong feature of chaotic system[12,13]. It describes the average exponential divergence rate of adjacent trajectories, which is defined as

$$\lambda_{\max} = \frac{1}{t_m - t_0} \sum_{n=1}^{N} \ln \frac{d(t_n)}{d(t_{n-1})} \tag{7}$$

Wherein $d(t_n)$ represents the distance between the nearest two points on track at t_n time.

2) Spectral entropy complexity

SEC[14,15] analyzes the proportion of different frequencies in the time sequence, and obtains firstly the spectrum of the signal through Fourier transform as in Formula 8:

$$Y_i = \frac{|\mathrm{FFT}(x_i)|^2}{N}, P_i = \frac{Y_i}{Y} \tag{8}$$

Wherein Y is sum of Y_i. The final definition is as Formula 9:

$$SEC = -\frac{\sum_{i=1}^{N} P_i \ln P_i}{\ln N} \tag{9}$$

3) Three metrics of spring test

The spring test[25] is the double group extension of the characterized time series obtained by hyperbolic tangent and its five threshold mapping. The *CC* (construction creep) index aims to characterize the self-similarity measuring results of the geometric instability of the one-dimensional manifold spring (test terms: 3*S* plot plus *CC* rate). After understanding the measure core of *CC* metric we introduce one rapid *CC* metric (*rCC*) embedded in extreme value searching strategy and another new rapid index of *CV* (chart variance) depicting the rotation phase feature of local chart (local coordinates) in the body of gained spring.

(a) *CC* index

The index of ***CC*** extracting the self-similarity of the spring body with the key definition formula is in Formula 10:

$$CC = \min\left\{\sum_{i=2}^{q} e_i^{m_1} /(m_1 \cdot (q-1))\right\} \times 100\% \tag{10}$$

Wherein e is the error accuracy[25], q=INT(N/m_1), m_1=2,3,⋯,INT(N/2).

(b) *rCC* index

The new index of rapid *rCC* simplifies *CC* by peak valley mapping, and the group with the most triaxial peak and valley values is actually selected as new simplified manifold of the spring in written:

$$s'(n') = \mathrm{minmax}\left\{s_\varphi(n)\right\} \tag{11}$$

Wherein $s_\varphi(n)$ is the spring manifold in the 3*S* plot, φ is a subset (axis) in {x, y, z}, and n' is the total number of peaks and valleys. Since the original spring manifold may have no peak and valley values, we define the final new simplified manifold as:

$$s''(n') = \begin{cases} s'(n'), & n' > 3 \\ s_\varphi(fi), & i = 1,2\Lambda\ c, n' \le 3 \end{cases} \tag{12}$$

When the numbers of peaks and valleys be less than 3, we set equidistant sampling in rate of f=INT(n/c), and c is an integer greater than 3. To co-work with Formulas 10, 11 and 12, we obtained *rCC* index.

(c) *CV* index

Another new index of *CV* uses cosine similarity to judge the periodic change (per chart) of the spring rotation property, and the intermediate formula is defined as:

$$CV' = \frac{1}{L-1}\sum_{k=1}^{L}(z_k - \mu_z)^2 \qquad (13)$$

Wherein z_k is the position difference where the cosine similarity between the kth point and the (k+1)th point be less than the key solid threshold R; L is the length of z_k sequence; μ_z is the mean value of z_k. In order to analyze the numerical significance, the data range of CV' is compressed as:

$$CV = \sqrt[4]{CV'} \qquad (14)$$

3. Test case types

The chaos data under test come from classical Chua's equation and the unified system (benchmark system). The novel discovered chaos signals are generated from 555-timer with one capacity feedback.

1) Chaos equations

Chua's equation ($a \in [2.8,3.5]$) is as[25]:

$$\begin{aligned} dx/dt &= -2.564x+10y+0.5a(|x+1|-|x-1|) \\ dy/dt &= x-y+z \\ dz/dt &= -14.706y \end{aligned} \qquad (15)$$

Five states of single period, double-period, three-period, single-scroll and double-scroll are located at parameter a=2.8,2.95,3.01,3.11,3.45.

Unified equation ($\beta \in [0,1]$) is as benchmark system[26]:

$$\begin{aligned} dx/dt &= (25\beta+10)(y-x) \\ dy/dt &= (28-35\beta)x - xz + (29\beta-1)y \\ dz/dt &= xy - (8+\beta)z/3 \end{aligned} \qquad (16)$$

Three narrow period windows are located at parameter β=0.37,0.47,0.58.

Experiment condition sets: Simulation software MATLAB2018b, CPU Intel (R) Core (TM) i5-3230M @2.6GHz; The test data are solved by the instruction ode45 for 6000 points (the initial value is [0.1,0.1,0.1], the step size is 0.01, and wherein the previous 3000 points are omitted).

2) 555-timer chaos

Figure 1 shows that three components (555-timer chip[27,28], resistor R1 and capacitor C1) can form a multi-vibrator. When we add a capacitor C2 in parallel of resistor R1, can we get the output of chaotic signal from chip pin3?

Experiment condition sets: DS4014E oscilloscope with 100 MHz bandwidth; Positive 5V power supply; The sampling rate is 5MHz, and the data length is 70000 points (the data is divided into 7 windows (segments).

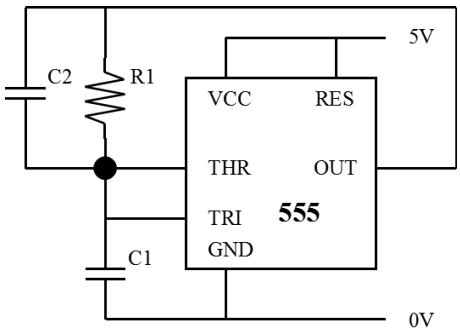

Fig. 1. 555-timer chaos circuit

Next we will demonstrate the limitations of the basic methods and the advantages of the new metrics of 3*S* plot, including main methods contrasting, our understandings and interpretations.

III. Results and Discussions

Figure 2 shows period three bifurcation diagram of Chua's equation following four basic features.

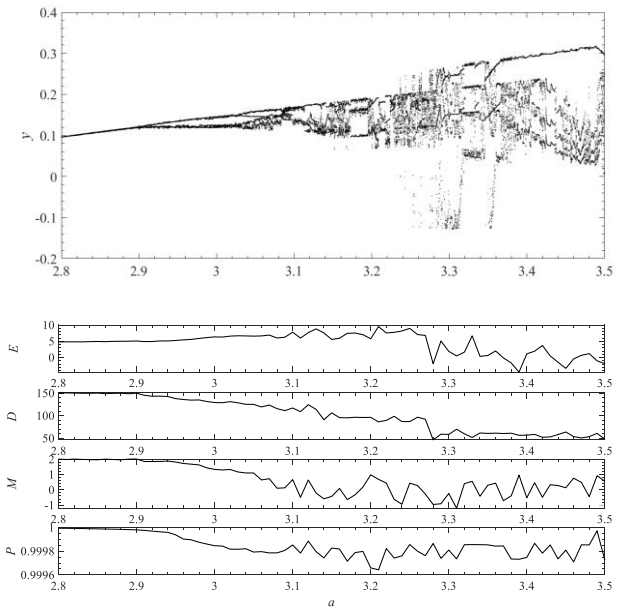

Fig. 2. Bifurcation diagram, track entropy E, Euclidean distance D, total variation of track M and total variation of track phase P for scanning the parameter a of chaos evolution of Chua's equation

Note 1: The four characteristic rules corresponding to the geometric intuition of bifurcation diagram are: Before trifurcation (a=3.01), the characteristics are monotonous and stable; After entering the single scroll (a=3.11), the characteristic fluctuations are obvious.

Note 2: Track entropy E lacks the excellent complex monotonicity of describing chaos, for the reason of unknown of probability distribution. The probability density function of map-typed chaos can be calculated using Frobenius-Perron operator[10], but FP operator exposes the weakness of cyclic definition of unknown measure.

Note 3: Euclidean distance D exists the excellent complex monotonicity while describing chaos, because of the sum of mean-removed track probability squares.

Note 4: Total variation of track M, as the essence of track probability measure, has the excellent complex monotonicity while describing chaos.

Note 5: Keeping the consistent recognition effect of chaos, total variation of track phase P uses only the 1000 points of track while other methods are with data lengths of 2000 points. Here the distinguishing sensitivity advantage of chaotic phase dynamics be preliminarily demonstrated.

But above methods cannot pass the united equation. So far we temper our spring test metrics, under the lights of two gold standards of *LE* with parameters and *SEC* without any parameter.

The first term of spring test is 3*S* plot, see Figure 3, it illustrates here three kinds of spring-shapes corresponding to states of order, chaos and random number, respectively.

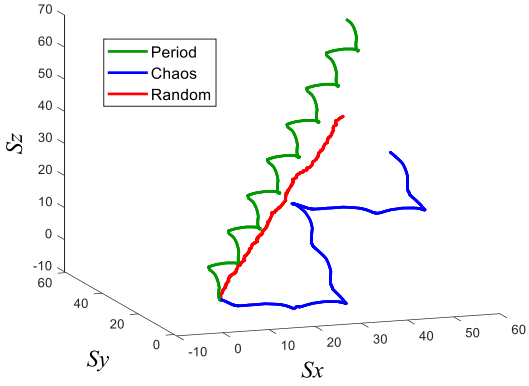

Fig. 3. 3*S* plot of spring test, green (good spring), single period state; blue (damaged spring), double-scroll chaos in Chua's equation; red (thin spring), pseudorandom number of Gaussian distribution

Note 1: Springs with different degrees of smoothness need specific measure indicators. The measuring principles concern both asymmetric attractor extracting by hyperbolic tangent map and noise depression with five thresholds.

Note 2: The second term of spring test is *CC* rate. The maximum values characterizing the monotone properties of random numbers are (1) $CC \approx rCC$=84.0; (2) *SEC*=0.94; (3) *LE*=2.1 (dimensional d=3; time delay τ=4). For diagnosing comparison criteria of random number, please see NIST SP800-22[29].

The complexity measuring results in Figure 4 are better than that in Figure 2.

Note 1: If an appropriate delay time parameter selected well exists (here τ=4), *LE* jumps from near zero on the negative side (order state) to a positive indicator (chaos).

Note 2: The advantage of *SEC* needs no manual parameter selection, but the premise is with data non-stationary and data length greater than 2000 points.

Note 3: The metric of *rCC* speeds up *CC* computing time as one order of magnitude, at the cost of indication value of order state rose by 15.

Note 4: Grasping spring rotation in 3*S* plot, *CV* (chart variance) finishes diagnosis work.

All new metrics of spring test proved the consistent identification results on bifurcation chaos evolution of Chua's equation, with data lengths of 2000 points.

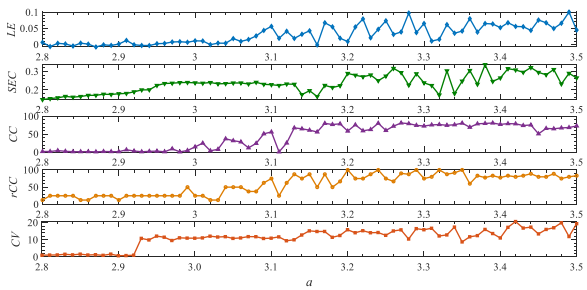

Fig. 4. Five features of *LE*, *SEC*, *CC*, *rCC* and *CV* for scanning the parameter *a* of the bifurcation chaos evolution of Chua's equation

We further test and verify the new indicators by benchmark system, the striking results are in Figure 5.

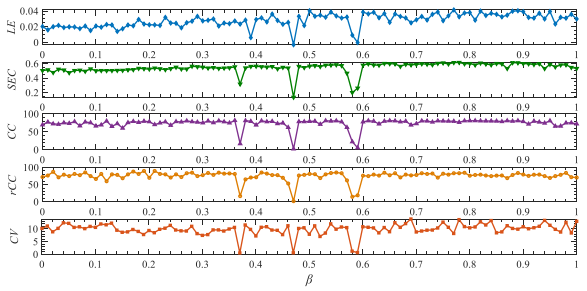

Fig. 5. Five features of *LE*, *SEC*, *CC*, *rCC* and *CV* for scanning the parameter β of unified equation with three period-valleys

Note 1: Three period-valleys are arranged in order, with delay time has to change into τ=20 for *LE* and the solid threshold value keeps on *R*=1.3 for *CV* index.

Note 2: Through cosine distance we further reduce the time consumption by one order of magnitude of *CV* index, approaching the time complexity of *SEC* with FFT instruction core.

Leaving the complexity identification of the benchmark system, we approached the 555 timer chip that shocked the world since 1971. As long as we added a capacitor C2 in parallel of R1 and then apply new metrics to distinguish chaos generating, we successfully found a new chaotic signal generator.

Combined with Figure 1, we gained Figure 6.

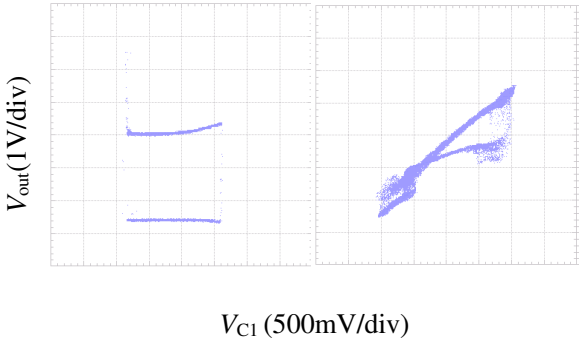

Fig. 6. Phase diagrams of 555-timer chaos (left, multi-vibrator; right, chaos)

Note 1: Figure 6 (left) shows symmetric waveforms with a few switching random noises in V_{out} inner chip 555.

Note 2: Figure 6 (right) illustrate chaotic state near number "8" memristor attractor.

Note 3: The differential capacitor C2 releases the broadband chaotic signal component in V_{out} (chaos state), and the mechanism of chaos starting is stochastic resonance induced by the noise component in V_{out} (multi-vibrator state).

Corresponding to Figure 6, we utilize five main tools to distinguish the outputs' states (multi-vibrator, chaos) in Figure 7.

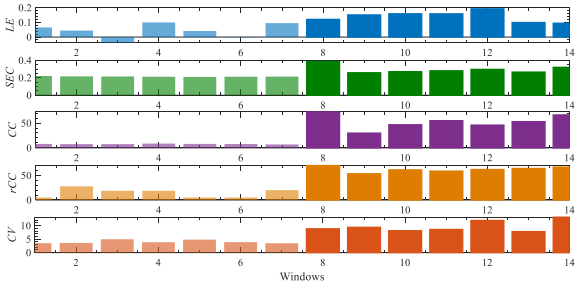

Fig. 7. Five features of 555-timer chaos (left window-1-7, multi-vibrator; right window-8-14, chaos)

Note 1: We contribute obviously the lower and higher levels of multi-vibrator and chaos by all five features. Three complexity metrics of spring test provide at least twice the difference. *LE* touches the negative period signs while *SEC* keeps stable states in all multi-vibrator windows.

Note 2: Here we must set the delay time τ=20 for *LE* and new solid threshold value R=0.5 for *CV* index.

Note 3: Among three metrics of spring test, only parameter R needs to operate manually. The auto-threshold law observed here is that equations submit to the ergodic property of track points in attractor space and one-dimensional time series be subject to the dimension upgrading strategy.

IV. Conclusions

It is a difficult computing work to extract manifolds quickly from chaotic attractors, which characterize the neighborhood boundary of fixed points. In sharp technical contrast to this cognition, we invent spring test for diagnosing time series (coming from equations or application scenarios) in test terms of 3S plot and its complexity measures coined construction creep (*CC*, in rang of 0~100) rate, rapid *CC* (in rang of 0~100) and chart variance (*CV*, in rang of 0~20).

The impressive chaos pattern recognition grasped the benchmark system of united equation and novel 555-timer chaotic circuit without inductor and in single power supply.

With our automatic spring testing technique, in future work we will face the confusion of lack of phase sensitive index in brain computer interface.

References

[1] T Ling, L Huiling, Y Fengmei, Y Lean, “Complexity testing techniques for time series data: a comprehensive literature review”, *Chaos Solitons and Fractals*, Vol.81, pp.117-135, 2015.

[2] G. Parisi, “Complex systems: a physicist's viewpoint”, *Physica A*, Vol.263, No.1-4, pp.557-564, 1999.

[3] L Deng, D Yu, *Deep Learning Methods and Applications*, China Machine Press, 2015.

[4] A. M. Turing, “The chemical basis of morphogenesis”, *Philosophcal Transactions of the Royal Society of London, Series B*, Vol.237, pp.37-72, 1952.

[5] N. H. Packard, J. Crutchfield, J. Famrmer, “Geometry from a Time Series”, *Physical Review Letters*, Vol.45, No.9, pp.712-716, 1980.

[6] E. T. Jaynes, “Information theory and statistical mechanics”, *Physical Review*, Vol.106, No. , pp.620-630, 1957.

[7] O. E. Rössler, C. Letellier, *Chaos*, Switzerland: Springer Nature, 2020.

[8] C. Diks, J. C. Houwelingen, F. Takens, J. DeGoede, “Reversibility as a criterion for discriminating time series”, *Physics Letters A*, Vol.201, No.2-3, pp.221-228, 1995.

[9] L. O. Chua, “Local activity is the origin of complexity”, *International Journal of Bifurcation and Chaos*, Vol.15, No.11, pp.3435-3456, 2005.

[10] G. Setti, G. Mazzini, R. Rovatti, S. Callegari, “Statistical modeling of discrete-time chaotic processes: basic finite-dimensional tools and applications”, *Proceedings of the IEEE*, Vol.90, No.5, pp.662-690, 2002.

[11] Z You，E. J. Kostelich, J. A. Yorke, “Calculating stable and unstable manifolds”, *International Journal of Bifurcation and Chaos*, Vol.1, No.3, pp.605-623, 1991.

[12] A. Wu, S. Cang, R. Zhang, Z. Wang, Z. Chen, “Hyperchaos in a conservative system with nonhyperbolic fixed points”, *Complexity*, pp.1-8, 2018.

[13] A. Wolf, J. B. Swif, H. L. Swinney, and J. A. Vastano, “Determining Lyapunov exponents from a time series,” *Physica D*: *Nonlinear Phenomena*, Vol. 6, No.3, pp.285-317, 1985.

[14] K. H. Sun, S. B. He, Y. He, L. Z. Yin, “Complexity analysis of

chaotic pseudo-random sequences based on spectral entropy algorithm", *Acta Phys. Sin.*, Vol.62, No.1, pp. 010501-8 , 2013.

[15] A. Abdelsamie, G. Janiga, D. Thévenin, "Spectral entropy as a flow state indicator", *International Journal of Heat and Fluid Flow*, Vol.68, pp.102-113, 2017.

[16] R. Delage, Y. Takayama, T. Biwa, "Bifurcation diagram of coupled thermoacoustic chaotic oscillators", *Chaos*, Vol.28, pp.083125-7, 2018.

[17] C. Tsallis, "Entropic nonextensivity: a possible measure of complexity", *Chaos Solitons and Fractals*, Vol.13, No.3, pp.371-391, 2002.

[18] P. Lamberti, M. Martin, A. Plastino, O. Rosso, "Intensive entropic non-triviality measure", *Phys. A*, Vol. 334, No.1-2, pp. 119-131, 2004.

[19] E Korczak-Kubiak, A. Loranty, R. J. Pawlak, "Measuring chaos by entropy for a finite family of functions", *Chaos*, Vol.30, pp.063138-7, 2020.

[20] R. Lopez-Ruiz, H. L. Mancini, X. Calbet, "A statistical measure of complexity", *Phys.Lett.A*, Vol.209, No.5-6, pp.321-326, 1995.

[21] H. Xiong ,P. Shang, J. He, Y. Zhang, "Complexity and information measures in planar characterization of chaos and noise", *Nonlinear Dynamics*, Vol.100, pp.1673-1687, 2020.

[22] C Soize, R. Ghanem, "Physical system with random uncertainties: chaos representations with arbitrary probability measure", *SIAM Journal on Scientific Computing*, Vol.26, No.2, pp.395-441, 2004.

[23] T. Yalcınkaya, Y. Lai, "Phase Characterization of Chaos", *Physical Review Letters*, Vol.79, No.20, pp.3885-3888, 1997.

[24] R. Follmann, E. E. N. Macau, "Phase detection of chaos", *Physical Review E*, Vol.83, pp.016209-1-6, 2011.

[25] J. Cai, Y. Li, W. Li, L. Li, "Two entropy-based criteria design for signal complexity measures", *Chinese Journal of Electronics*, 2019, Vol.28, No.6, pp.1139-1143, 2019.

[26] Jinhu Lü, Guanrong Chen, "A new chaotic attractor coined", *International Journal of Bifurcation and Chaos*, Vol.12, No.3, pp.659-661, 2002.

[27] B. Santo, "25 microchips that shook the world", *IEEE Spectrum*, Vol.46, pp.34-43, 2009.

[28] M. Santillán, "Synchronization dynamics of two mutually coupled 555-IC based electronic oscillators", *Revista Mexicana de Fisica*, Vol.64, pp.107-115, 2018.

[29] State Password Administration, *GM/T0005-2012 Randomness Test Specification*, Chinese Standard Press, 2012.

[30] S. Fauve, F. Heslot, "Stochastic resonance in a bistable system", *Physics Letters A*, Vol.97, pp.5-7, 1983.

Declarations

1. Funding

"This work was supported by Technological Innovation of Key Industries in Suzhou City Prospective Application Study (Grant numbers [SYG201701]) and Postgraduate Research & Practice Innovation Program of Jiangsu Province [grant number KYCX18_2509].

2. Competing Interests

The authors have no relevant financial or non-financial interests to disclose.

3. Author Contributions

All authors contributed to the study conception and design. Material preparation, data collection and analysis were performed by Jie Cheng, Haiyong Huang and Wenshi Li. The first draft of the manuscript was written by Jie Cheng and all authors commented on previous versions of the manuscript. All authors read and approved the final manuscript.

4. Data Availability

The datasets generated during and/or analysed during the current study are not publicly available due to privacy restrictions but are available from the corresponding author on reasonable request.